Am. J. Hum. Genet. 73:791–800, 2003

Mutations in the Gene Encoding Capillary Morphogenesis Protein 2 Cause Juvenile Hyaline Fibromatosis and Infantile Systemic Hyalinosis

Sandra Hanks,[1] Sarah Adams,[1] Jenny Douglas,[1] Laura Arbour,[2] David J. Atherton,[3] Sevim Balci,[7] Harald Bode,[8] Mary E. Campbell,[4] Murray Feingold,[9] Gökhan Keser,[10] Wim Kleijer,[11] Grazia Mancini,[11] John A. McGrath,[5] Francesco Muntoni,[6] Arti Nanda,[12] M. Dawn Teare,[13] Matthew Warman,[14] F. Michael Pope,[4] Andrea Superti-Furga,[15] P. Andrew Futreal,[16] and Nazneen Rahman[1]

[1]Section of Cancer Genetics, Institute of Cancer Research, Sutton, Surrey, United Kingdom; [2]Department of Medical Genetics, University of British Columbia, Vancouver; [3]Paediatric Dermatology, Great Ormond Street Hospital for Children, [4]Connective Tissue Matrix Genetics Group, Division of Life Sciences, King's College London, [5]Department of Cell and Genetic Skin Disease Group, St John's Institute of Dermatology, Division of Skin Sciences, The Guy's, King's College and St Thomas' Hospitals' Medical School, and [6]Department of Paediatrics, Dubowitz Neuromuscular Centre, Imperial College, London; [7]Clinical Genetics Unit, Hacettepe University, Ankara; [8]Sozialpadiatrisches Zentrum der Universitats-Kinderklinik, Ulm, Germany; [9]National Birth Defects Center, Waltham, MA; [10]Department of Rheumatology, Ege University, Izmir, Turkey; [11]Department of Clinical Genetics, Erasmus Medical Center, Rotterdam; [12]As'ad Al-Hamad Dermatology Center, Al-Sabah Hospital, Kuwait; [13]Mathematical Modelling and Genetic Epidemiology Group, University of Sheffield, Sheffield; [14]Howard Hughes Medical Institute, Department of Genetics and Center for Human Genetics, Case Western Reserve University, Cleveland; [15]Division of Molecular Pediatrics, Centre Hospitalier Universitaire Vaudois, Lausanne, Switzerland; and [16]Cancer Genome Project, The Wellcome Trust Sanger Institute, Hinxton, Cambs, United Kingdom

Juvenile hyaline fibromatosis (JHF) and infantile systemic hyalinosis (ISH) are autosomal recessive conditions characterized by multiple subcutaneous skin nodules, gingival hypertrophy, joint contractures, and hyaline deposition. We previously mapped the gene for JHF to chromosome 4q21. We now report the identification of 15 different mutations in the gene encoding capillary morphogenesis protein 2 (*CMG2*) in 17 families with JHF or ISH. CMG2 is a transmembrane protein that is induced during capillary morphogenesis and that binds laminin and collagen IV via a von Willebrand factor type A (vWA) domain. Of interest, CMG2 also functions as a cellular receptor for anthrax toxin. Preliminary genotype-phenotype analyses suggest that abrogation of binding by the vWA domain results in severe disease typical of ISH, whereas in-frame mutations affecting a novel, highly conserved cytoplasmic domain result in a milder phenotype. These data (1) demonstrate that JHF and ISH are allelic conditions and (2) implicate perturbation of basement-membrane matrix assembly as the cause of the characteristic perivascular hyaline deposition seen in these conditions.

Introduction

Juvenile hyaline fibromatosis (JHF [MIM 228600]) is an autosomal recessive condition that usually presents with nodular/papular skin lesions and gingival hypertrophy during the first few years of life. The skin lesions typically occur on the hands, scalp, and ears and around the nose and require recurrent excision. Progressive joint contractures and osteopenia are characteristic and may result in severe limitation of mobility. The diagnosis is confirmed by demonstration of hyaline deposition in the dermis (Keser et al. 1999; Mancini et al. 1999; Allen 2001; Rahman et al. 2002). The origin and nature of the amorphous hyaline material have been unclear, but it appears to be principally composed of glycoproteins and glycosaminoglycans (Ishikawa et al. 1979; Mayer-da-Silva et al. 1988).

Infantile systemic hyalinosis (ISH [MIM 236490]) is an autosomal recessive condition that shares many similarities with JHF. Clinical presentation is usually at birth or within the first few months, with painful, swollen joint contractures and livid red hyperpigmentation over bony prominences. Pearly papules (predominantly of the face, scalp, and neck) and fleshy nodules (particularly in the perianal region) then develop. Gingival hypertrophy and thickened skin are also characteristic features. Osteopenia is often present and results in increased susceptibility to bone fractures. Affected children are susceptible to infections and/or intractable diarrhea due to protein-losing enteropathy, and many die in infancy from resulting multisystem failure. Children with ISH are intellectually normal; if they survive infancy, they become less susceptible to infection, and their joints may become less painful. However, their

Received May 28, 2003; accepted for publication July 9, 2003; electronically published August 21, 2003.

Address for correspondence and reprints: Dr. Nazneen Rahman, Section of Cancer Genetics, Brookes Lawley Building, Institute of Cancer Research, 15 Cotswold Road, Sutton, Surrey, SM2 5NG, United Kingdom. E-mail: nazneen@icr.ac.uk

0002-9297/2003/7304-0008$15.00

mobility remains severely restricted by joint contractures. Histologically, ISH is also characterized by hyaline deposition, but this is more widespread than in JHF and can affect many tissues, including skin, skeletal muscle, cardiac muscle, gastrointestinal tract, lymph nodes, spleen, thyroid, and adrenal glands (Landing et al. 1986; Glover et al. 1991, 1992; Sahn et al. 1994; Stucki et al. 2001).

The underlying pathogenesis of JHF and ISH was previously unknown. In the past, these conditions have been postulated to be lysosomal storage disorders (Nezelof et al. 1978), disorders of abnormal collagen metabolism (Kayashima et al. 1994; Lubec et al. 1995; Breier et al. 1997), or the result of defective glycosaminoglycan formation (Kitano et al. 1972; Iwata et al. 1980; Remberger et al. 1985; Breier et al. 1997). However, no consistent biochemical abnormalities in support of any of these hypotheses are reliably present (Stucki et al. 2001).

We previously mapped the gene that causes JHF to a 7-cM interval on chromosome 4q21 in five families (Rahman et al. 2002). We hypothesized that ISH is due to the same gene as is JHF, and we ascertained and analyzed 11 families with ISH for linkage to chromosome 4q21. These analyses confirmed that JHF and ISH are allelic and refined the gene interval to 0.85 Mb. Mutation analysis of genes within the minimal interval revealed that deleterious mutations in the gene encoding capillary morphogenesis protein 2 (*CMG2*) were the cause of both conditions.

Subjects and Methods

Subjects

Approval for the study was obtained from the London Multicentre Research Ethics Committee, and informed consent was given by all families. In total, 8 families (A–H) with a clinical diagnosis of JHF and 10 families (I–R) with a diagnosis of ISH were ascertained. Cases of JHF were characterized by (1) diagnosis after birth, typically after 18 mo, (2) joint contractures, (3) nodular and/or papular skin lesions, (4) gingival hypertrophy, and (5) histological evidence of hyaline deposition in the dermis. Cases of ISH were characterized by (1) onset at birth or in the first few months of life, (2) joint contractures, (3) painful diffusely thickened skin, often with hyperpigmentation over joints, (4) papular and/or nodular skin lesions, (5) gingival hypertrophy, (6) visceral involvement, and (7) histological evidence of hyaline deposition. Clinical and histological details from several of these families have been published previously: families A, B, and E (Rahman et al. 2002); family C (Keser et al. 1999); families D and F (Mancini et al. 1999); family G (Balci et al. 2002); family H (Richter et al. 1999); family L (Stucki et al. 2001); and family Q (Glover et al. 1992). Control samples were obtained from Human Random Control DNA panels from the European Collection of Cell Cultures.

Microsatellite Analysis

DNA was extracted from peripheral blood samples, using standard procedures. We identified known chromosome 4q21 markers, using the Marshfield Clinic database (see the Center for Medical Genetics Web site) and the University of California–Santa Cruz (UCSC) Human Genome Project Working Draft sequence (see the UCSC Genome Bioinformatics Web site). We generated new markers by searching the 7-cM interval encompassing the JHF gene for dinucleotide, trinucleotide, and tetranucleotide repeat elements, and we designed amplifying primers, using Primer3 software (table A [available online only]). We identified 20 novel microsatellite markers that we called "SH-REPs" (systemic hyalinosis repeats). The order and physical positions of the known and newly generated markers analyzed are shown in figure 1. The microsatellite markers were radiolabeled and PCR amplified in the families with JHF and ISH, and the resulting PCR products were electrophoresed through 6% denaturing polyacrylamide gels before exposure to x-ray film.

Mutation Analysis

Amplifying primers flanking the exons and the intron-exon boundaries of the 17 *CMG2* exons were designed using Primer3 software. The primer sequences and sizes are shown in table 1. Using a Touchdown 68°C–50°C protocol, we amplified all products apart from exon 8, for which the PCR was performed at a single annealing temperature, of 55°C. We used conformation-sensitive gel electrophoresis (CSGE) (Ganguly et al. 1993) to mutationally screen *CMG2* in the 18 families. Genomic DNA from cases showing mobility shifts on CSGE was bidirectionally sequenced using the BigDyeTerminator Cycle Sequencing Kit and a 3100 automated sequencer (ABI Perkin Elmer). The mutations were numbered from the first ATG (methionine) of the full-length *CMG2* (GenBank accession number AK091721), with A as nucleotide 1. For evaluation of the likely pathogenicity of missense and in-frame alterations, we screened 300 control subjects from the United Kingdom. Owing to the wide diversity of ethnic groups included in the study, it was not feasible to obtain sufficient numbers of ethnically matched control subjects for individual mutations. To confirm the *CMG2* cDNA sequence and the pathogenicity of splice-site mutations in families A and C, cDNA was synthesized from RNA extracted from fibroblast cell lines, using standard procedures. *CMG2* cDNA was sequenced in two fragments, using over-

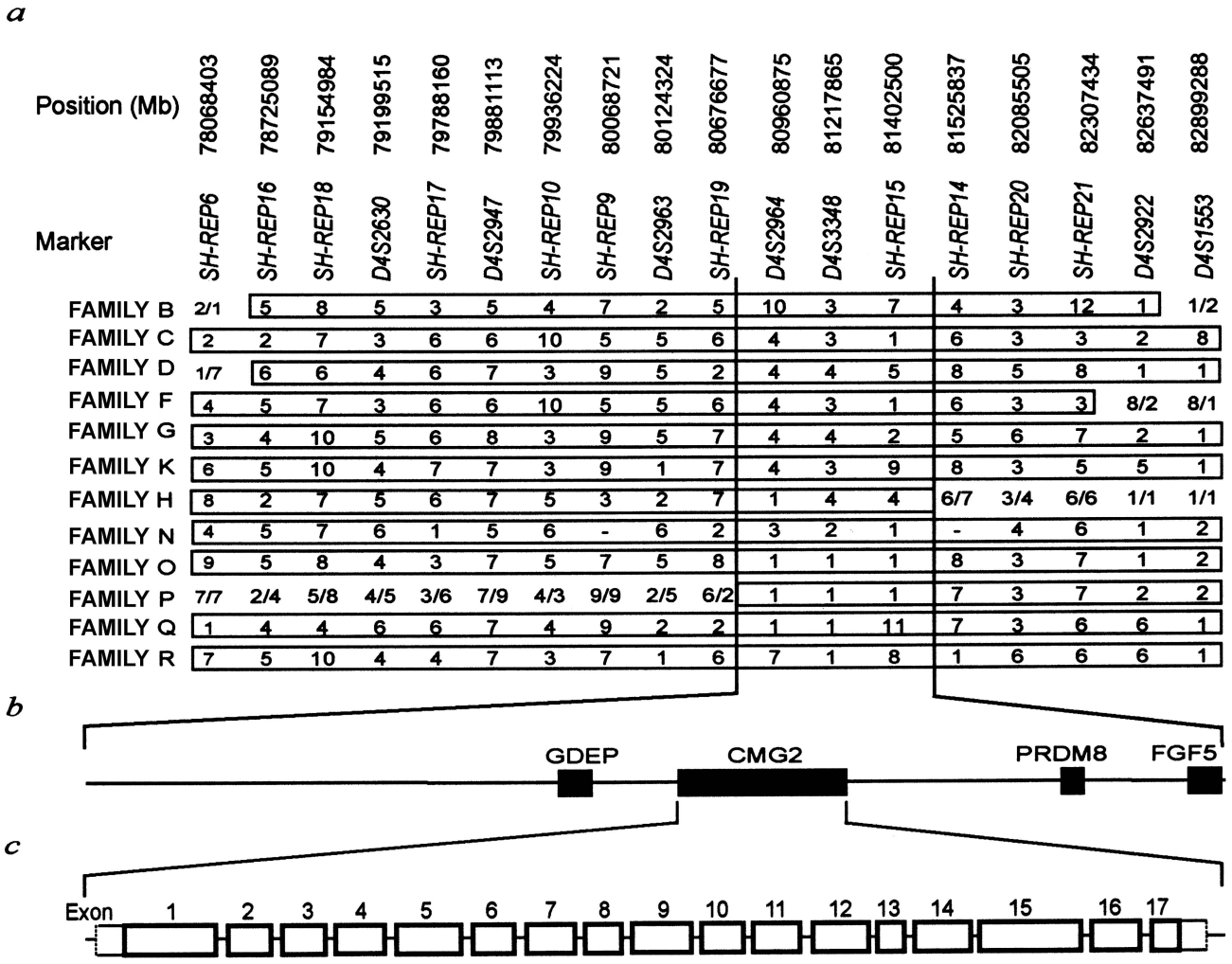

Figure 1 Homozygosity mapping and genomic structure of *CMG2*. *a*, Homozygosity-mapping data from 18 microsatellite markers on chromosome 4q21 in consanguineous families with JHF and ISH, showing marker alleles, regions of homozygosity (*boxed*), and key recombination events in families H and P. The physical distances of the markers according to the November 2002 UCSC Human Genome Project Working Draft (see the UCSC Genome Bioinformatics Web site) are shown above each marker. *b*, Partial transcript map (drawn to scale) of the critical interval, showing currently known genes. *c*, Genomic structure of full-length *CMG2*.

lapping primer pairs: CMG2-1F (5′-ACAGCAACTTGCGGAGAGAT-3′) and CMG2-1R (5′-TGCAGAGAACACTGCCATTC-3′); and CMG2-2F (5′-GTGGGGGAGGAATTTCAGAT-3′) and CMG2-2R (5′-CCTCAACAAAGCCCAGAGAG-3′).

Expression Analysis

RT-PCR analysis was performed in duplicate on normalized multiple-tissue cDNA panels 1 and 2 (Clontech), using primers 5′-ACAGCAACTTGCGGAGAGAT-3′ and 5′-AAGCAAAGCAGAAGGCAGAG-3′, which amplify exons 2–17 of *CMG2*. The recommended Titanium *Taq* DNA polymerase was used with a Touchdown protocol 68°C–50°C for 18 cycles, followed by 14 cycles with annealing at 50°C. Five microliters of product was analyzed by agarose gel electrophoresis with ϕX-174 *Hae*III digest size marker.

Bioinformatic Analyses

CMG2 cDNAs were identified from GenBank and Ensembl and were aligned against each other, using ClustalW, and against genomic sequence, using BLAT (see the Human BLAT Search Web site). The related human protein, tumor endothelium marker 8 (TEM8), and orthologous proteins in rat, mouse, and fugu were identified using BLAST. The novel cytoplasmic domains from pig, cow, and zebrafish were

Table 1

Primer Pairs Used to Amplify the *CMG2* Coding Sequence and Sizes of PCR Products

Exon	Primer Sequence (5′→3′)		Size (bp)
	Forward	Reverse	
1	GCTGTGGCTGTTGGTGCT	GCTTGCCCTTTGAAAGAAGA	249
2	TTCCGTGTTTTGTTTCTCTGA	CAATACGACCTTGAGGCACTT	245
3	AGCCTGGACCATTCAGTGAG	ATTCCACTGAGAGGCCTGAA	284
4	TGTTACCTTTGCTCTTTGCTCA	TGAGCTTTGCTAGAGGGTTTT	213
5	GCTTGATGGAACATGCTGGT	AGCGATGTACAGTGGGGTGT	224
6	CTTTCTCCCTCTCCCCTCTC	AACAATCGACCAGTGTCACAA	229
7	TTGTATGTGTCAGCCACTCCTT	TAATGACCACCTGCACTGGA	225
8	TGGAGAAGACCTCAAGGTTATTA	TTCTTTTTCCAACATGAGTTTCA	249
9	CTTTCATTTCAGCTTGTGTTTTT	TGTCAGTTAGTTTTCGTTGGAGA	268
10	TCCACATTTGAACTCTGATTGA	TGACCAATGTATATGTCACCATTTT	250
11	TGTTTTCTGGCTGGTTTTGA	TTTCTGGATGGAATTGCTTTT	229
12	TTCTGAATTATTTTCTGGTGTTTCC	TGGCATTTATTCATATTTCAGACC	276
13	GCAAGCTTCAGTGAGGGACT	GCATGGTATCTGCATTTGGA	230
14	TGAGCCAGTTCCGACTAAACA	TGGCTTAATAGCCCTAGAAATACAT	229
15	GCCTGTTCCTCTAGGACACTTT	GGGGGATGTGGTACAAAAA	300
16	TCTTCGTTTTATGTCTTCATTTATTCA	TCCCTGCCTCCATTATACTGAC	227
17	GGAAAACTAGATGTTCTCATGCTTT	CATTTCCCGACTGAGAGGAA	247

identified with tblastn, using the CMG2 protein sequence against the National Center for Biotechnology Information Expressed Sequence Tags Database, translated in all six frames. Those sequences showing homology in one reading frame were aligned using MultAlin and ClustalW. The Pfam, Prosite, and Conserved Domain databases were searched for sequences similar to the CMG2/TEM8 cytoplasmic domain.

Results

Homozygosity Mapping in JHF and ISH Cases to Refine the Gene Interval

We previously mapped the gene for JHF to a 7-cM interval between D4S2393 and D4S395 (Rahman et al. 2002). To refine this interval, we developed new microsatellite markers. Analyses of these markers in the original families with JHF reduced the gene interval to a 5-Mb region between SH-REP6 and D4S1553 (data not shown). We analyzed the 18 known and newly generated markers within this interval in 12 families with JHF and ISH that were either known or suspected to be consanguineous. All analyzed families were homozygous at multiple markers within the region, consistent with linkage of both JHF and ISH to chromosome 4q21. The regions of homozygosity in families H and P refined the interval encompassing the gene to 0.85 Mb between SH-REP19 and SH-REP14 (fig. 1*a*). The minimal region contained four known genes—*GDEP, CMG2, PRDM8,* and *FGF5* (fig. 1*b*). We screened *FGF5* but did not identify any likely pathogenic mutations (data not shown).

Identification of a Novel Cytoplasmic Domain in the Full-Length CMG2

CMG2 is a transmembrane protein with a von Willebrand factor type A (vWA) domain in the extracellular region. CMG2 was reported elsewhere as a 386-amino-acid protein expressed only in placenta (Bell et al. 2001). However, alignment of *CMG2* cDNAs and genomic sequence suggested that a 1.46-kb ORF that includes four extra exons (8–11) between the vWA domain and the transmembrane domain represents the full-length gene (fig. 1*c*). This transcript is predicted to encode a 488-amino-acid protein, which we confirmed by RT-PCR and cDNA sequencing (fig. 2*a*). By RT-PCR of human cDNA multiple-tissue panels, expression of the transcript was demonstrated in all tissues analyzed except brain (fig. 2*b*).

The only known paralog of CMG2 is TEM8, which shows 56% overall amino acid identity (Scobie et al. 2003). Sequence comparison of CMG2 and TEM8 revealed that the highest level of conservation (80%) occurred at residues 338–421 in the intracellular region of the protein. Within this cytoplasmic domain, we identified a novel 50-amino-acid motif (residues 367–417) that was almost identical in both human proteins and orthologs in cow, pig, chicken, mouse, rat, fugu, and zebrafish (fig. 3). The conserved cytoplasmic domain did not show significant similarity to any known pro-

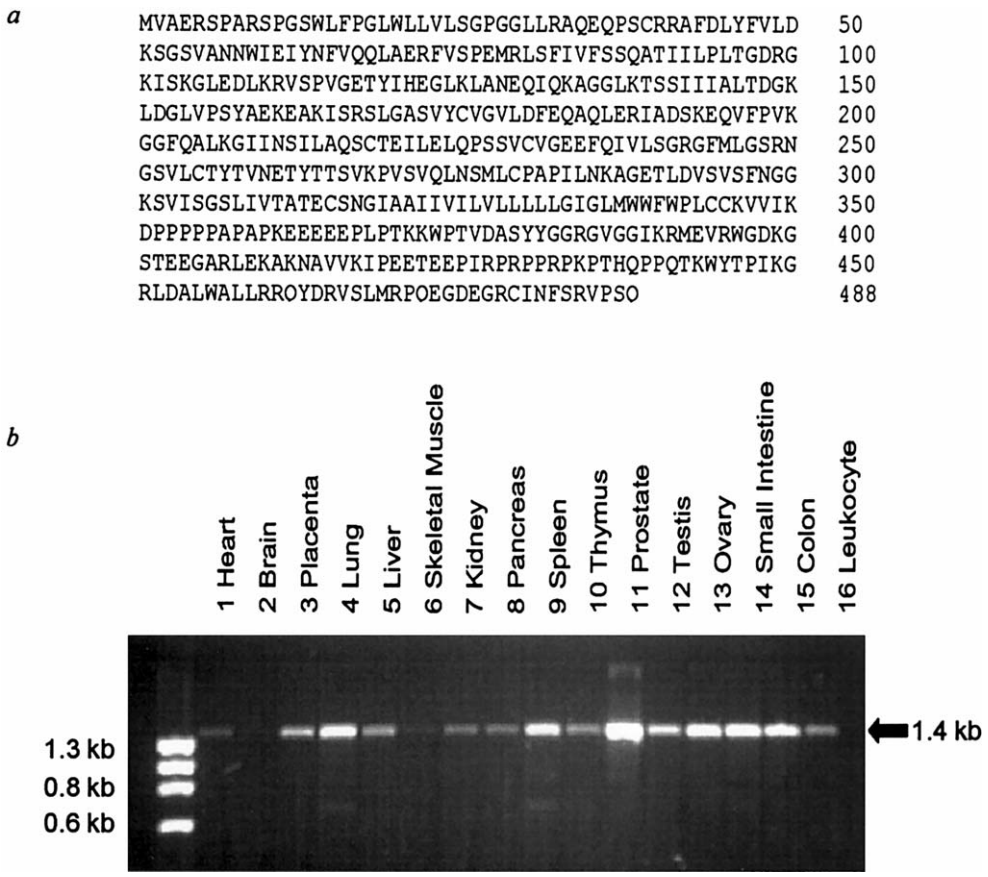

Figure 2 Expression of *CMG2*. *a*, Sequence of full-length CMG2. *b*, RT-PCR of human cDNA multiple-tissue panel (Clontech), showing expression of ~1.4 kb transcript in all tissues, except brain.

tein motifs in the Pfam, Prosite, or Conserved Domain databases.

Identification of CMG2 *Mutations in JHF and ISH Cases*

Genomic DNA from 18 families was screened for *CMG2* mutations by CSGE and direct sequencing. We identified 15 different mutations in 17 families (table 2 and fig. 4*a*). These mutations were predicted to abrogate CMG2 function and consisted of four small insertions or deletions, four mutations that alter consensus splice-junction sequences, one nonsense mutation, one in-frame insertion of a glutamine residue, and four nonconservative missense mutations. Using RT-PCR, we confirmed the pathogenicity of two splice-site mutations: IVS13+1G→A, which leads to an insertion of 4 bases after exon 13 and a translational frameshift (fig. 4*b*); and 1707G→A, a synonymous substitution that alters a consensus splice-junction base, resulting in an in-frame deletion of exon 14. The missense mutations were not present in 300 U.K. control subjects and occurred at residues conserved in both the mouse ortholog and the human paralog, TEM8 (data not shown). Moreover, these mutations were present in families in which homozygosity was present throughout the linked interval or in which a truncating mutation on the other allele was identified, indicating that *CMG2* is the causative gene in these families (table 2). We did not find a mutation in family O, but, because the case subject is homozygous at all of the chromosome 4q21 markers analyzed, it is presumed that abrogation of CMG2 function has caused ISH in this family (fig. 1*a*). Only one heterozygous mutation was identified in families E, J, and M. We assume that a second *CMG2* mutation is present in these families but was not detected, either because of lack of sensitivity of the screening technique or because the deleterious alterations are not detectable by our methods—for example, genomic rearrangements or regulatory mutations. It is possible that these cases are compound heterozygotes for mutations in two separate genes, but there is currently no evidence to support genetic het-

Figure 3 Sequence alignment of 50 amino acids in cytoplasmic domain of CMG2 and TEM8 in various species, showing high conservation. Black background indicates identical residues, and gray background indicates conservative substitutions. In pig, sheep, chicken, and zebrafish, the gene that the conserved region is from is currently unknown, because the full-length gene sequence is not available. The position of the missense mutation in family D is indicated by an arrow.

erogeneity in JHF or ISH, with all of the families thus far analyzed showing linkage and/or mutation evidence in support of *CMG2* as the causative gene. Identical founder mutations in families A and B and families C and F were identified, consistent with the chromosome 4q21 haplotype data (fig. 1*a*). Conversely, although a cytosine insertion in a poly-C tract in exon 13 was identified in three separate families, we believe these to have arisen independently, because the families carry different chromosome 4q21 haplotypes and *CMG2* polymorphisms. Moreover, two further families had different mutations involving the poly-C tract, which appears to be a mutational hotspot, presumably owing to the repetitive sequence (table 2). The mutations segregated with the disease in all families in which this could be evaluated, and all tested parents of case subjects were carriers, as expected in an autosomal recessive condition. We identified nine *CMG2* sequence variants that (*a*) did not segregate with the disease, (*b*) were present in individuals with two pathogenic mutations, and/or (*c*) led to intronic changes, and these were assumed to be innocuous polymorphisms (table 3).

Genotype-Phenotype Analyses

We compared the phenotypes of 14 cases in which *CMG2* mutations on both alleles were identified (table 2). All cases exhibited hyaline deposition, gingival hypertrophy, and skin nodules/papules. Missense and truncating mutations in the extracellular vWA domain were associated with a severe phenotype, typically presenting at birth, characterized by death in infancy from sepsis, intractable diarrhea, and/or multiorgan failure. Case subjects with at least one insertion/deletion mutation resulting in a translational frameshift all had the infantile form of the disease. Conversely, in-frame and missense mutations in the cytoplasmic domain were associated with a milder JHF phenotype, presenting in infancy, characterized by survival to adulthood without recurrent infections, gastrointestinal disease, or failure to thrive (fig. 1*a* and table 2). In particular, the tendoarticular manifestations, which are the predominant cause of morbidity for those who survive infancy, were extremely variable. This was exemplified by missense mutations in the vWA domain that resulted in severely limiting painful contractures (families L and R), whereas a missense mutation in the cytoplasmic domain resulted in no skeletal limitation (family D).

Discussion

CMG2 was originally identified as a gene upregulated in endothelial cells induced to undergo capillary formation in three-dimensional collagen matrices (Bell et al. 2001). CMG2 is a type 1 transmembrane protein, and its extracellular region contains a vWA domain that shows strong binding to laminin and collagen IV, both of which are markedly induced in endothelial cell morphogenesis in a time frame coincident with CMG2 induction (Bell et al. 2001). These data implicate CMG2 in basement-membrane matrix assembly and endothelial cell morphogenesis and suggest that the hyaline material deposited between the endothelial cells and pericytes in ISH and JHF may result from leakage of plasma components through the basement membrane to the perivascular space.

Preliminary genotype-phenotype analyses suggest that the wide phenotypic variability associated with CMG2 abrogation may be related, at least in part, to the underlying mutational spectrum. The milder JHF cases were associated with in-frame and missense mutations within the novel cytoplasmic domain. In contrast, cases in which vWA-domain binding is predicted to be impaired typically exhibited a more severe form of the disease. These

Table 2

***CMG2* Mutations and Clinical Features of JHF and ISH Cases**

	Mutation			Phenotype									
Family (Ethnicity, Origin)	Nucleotide Change	Location	Mutation Effect	Status[a]	Diagnosis	No. of Affected Individuals	Age at Onset <6 mo	Skin Nodules	Gum Hypertrophy	Contractures	Failure to Thrive	Diarrhea	Infections
A (India)	1707G→A	Exon 14	Deletion	Hom	JHF	3	−	+	+	+	−	−	−
B (India)	1707G→A	Exon 14	Deletion	Hom	JHF	1	−	+	+	+	−	−	−
C (Western Turkey)	IVS13+1G→A	IVS13	Frameshift	Hom	JHF	2	−	+	+	+	−	−	−
D (Morocco)	1670A→G	Exon 14	Y381C	Hom	JHF	2	−	+	+	−	−	−	−
E (European)	IVS9+2T→C	IVS9	Splice defect[b]	Het	JHF	1	+	+	+	+	−	u	−
F (European)	IVS13+1G→A	IVS13	Frameshift	Hom	JHF	1	+	+	+	++	−	−	−
G (Eastern Turkey)	1404-1405insCAA	Exon 11	insQ293	Hom	JHF	3	+	+	+	++	−	−	−
H (Turkey)	IVS14+5G→T	IVS14	Splice defect[b]	Hom	JHF	1	+	+	+	++	−	−	−
I (European, Canada)	1678C→T	Exon 14	R384X	Het	ISH	1	+	+	+	++	+	+	+
	IVS8+1G→A	IVS8	Splice defect[b]	Het									
J (China)	1601-1602insC	Exon 13	Frameshift	Het	ISH	1	+	+	+	++	+	+	+
K (Fiji/East India)	1180T→C	Exon 8	C218R	Hom	ISH	3	+	+	+	++	+	+	+
L (European, Swiss)	1094T→C	Exon 7	I189T	Het	ISH	2	+	+	+	++	+	+	+
	1601-1602insCC	Exon 13	Frameshift	Het									
M (Puerto Rico + African American)	1601-1602insC	Exon 13	Frameshift	Het	ISH	1	+	+	+	++	+	+	+
N (Morocco)	1023–1024insA	Exon 6	Frameshift	Hom	ISH	2	+	+	+	++	+	+	+
O (Pakistan)				Hom	ISH	1	+	+	+	++	+	+	+
P (Hispanic, United States)	1601–1602insC	Exon 13	Frameshift	Hom	ISH	1	+	+	+	++	+	+	−
Q (Kuwait)	1602delT	Exon 13	Frameshift	Hom	ISH	2	+	+	+	++	+	+	+
R (Bedouin)	662T→C	Exon 1	L45P	Hom	ISH	2	+	+	+	++	+	+	+

Note.—+ = Present; ++ = severe; − = not present; u = unknown.

[a] Hom = homozygous for mutation; Het = heterozygous for mutation.

[b] The exact pathogenic effect of these splice-site mutations has not been demonstrated.

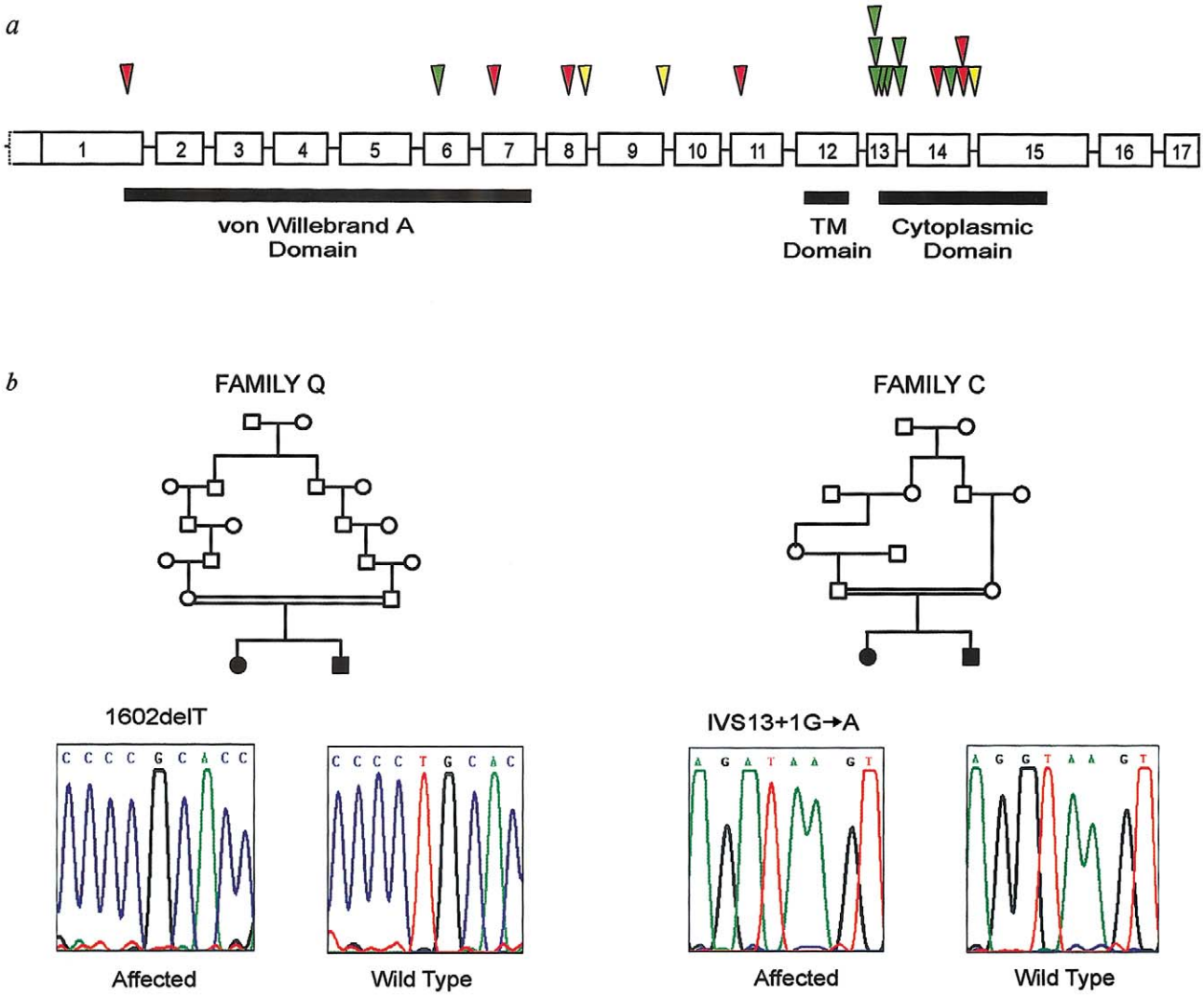

Figure 4 Genomic structure, protein domains, and mutation analysis of *CMG2*. *a*, Genomic structure and mutations in *CMG2* with the exon sizes drawn to scale and the position of functional and conserved domains indicated (TM = transmembrane). The 5′ and 3′ UTRs are indicated by open boxes and are not drawn to scale. Introns are also not drawn to scale. The approximate positions of identified mutations are given, with identical mutations shown above each other. Green triangle = mutation resulting in premature truncation due to either small insertion/deletion/nonsense or splice-site alterations; red triangle = in-frame alterations due to either missense base substitutions or in-frame insertion/deletion; yellow triangle = splice-site mutations in which the precise pathogenic effect has not been identified. *b*, Pedigree structure and mutations in selected families with JHF and ISH, showing wild-type and mutant *CMG2* sequence. The splice-site mutation in family C results in insertion of 4 bases and a frameshift.

data suggest that tissue-specific and/or domain-restricted differences in CMG2 function may exist. However, there is also evidence that mutation class and position are not sufficient to account for all clinical variability, since cases in families C and F that are homozygous for the same founder mutation (IVS13+1G→A) that results in a translational frameshift have somewhat different clinical phenotypes. Family C consists of two living affected individuals who presented with gingival hypertrophy and dermal lesions in childhood but developed significant locomotor problems only in adolescence (Keser et al. 1999). Family F harbors the same mutation as does family C and comprises a single case subject. This subject developed gingival hypertrophy and perianal papules at 6 mo with joint swelling and limitation developing at 9 mo; she was never able to walk but had no evidence of systemic disease typical of ISH, such as recurrent infections or gastrointestinal symptoms (Mancini et al. 1999). Clearly, detailed clinical histories from additional cases with confirmed mutations are required, to evaluate these putative genotype-phenotype associations, before meaningful conclusions can be drawn.

The only known human gene that shows strong homology to *CMG2* is *TEM8*. *TEM8* was original-

Table 3

Polymorphisms in *CMG2*

Location	Nucleotide Change	Protein Change
Intron 2	IVS2-43T→A	
Intron 2	IVS2-4G→A	
Intron 4	IVS4+8A→C	
Intron 6	IVS6+29A→C	
Intron 7	IVS7+54T→A	
Exon 13	1597C→G	P357A
Intron 13	IVS13-15A→G	
Exon 16	1923G→A	R465R
3′ UTR	2023C→T	

ly identified as a gene differentially expressed in tumor, as compared with normal colonic vasculature, and is thus of potential interest as a target for anti-angiogenic therapies in cancer (St Croix et al. 2000). It is currently unknown whether *CMG2* is similarly differentially expressed in tumor tissues. Intriguingly, both TEM8 and CMG2 have been shown to function as anthrax toxin receptors (Bradley et al. 2001; Scobie et al. 2003). Furthermore, in an in vitro system, a soluble version of the CMG2 vWA domain has been shown to act as a potent antitoxin, suggesting that CMG2 may prove useful in the development of anti-anthrax treatments (Scobie et al. 2003). Our data give the first insights into the in vivo role of CMG2 and may be of relevance in understanding the role of CMG2—and, possibly, the role of TEM8—in basement-membrane matrix processing, tumor angiogenesis, and anthrax toxicity, which understanding may in turn facilitate the therapeutic exploitation of these proteins. Moreover, we have identified a novel cytoplasmic domain that is the defining sequence hallmark of this protein family. The function of this domain is unknown, but the demonstration that in-frame deletions and missense mutations restricted to the domain are pathogenic indicates an important role that merits further investigation.

In conclusion, we have demonstrated that deleterious mutations in *CMG2* cause both JHF and ISH. These data provide the basis for diagnostic testing and genetic counselling for families and will lead to better understanding of the disease pathogenesis, which may in turn help reduce the high morbidity and mortality associated with these hyaline-deposition disorders.

Acknowledgments

We thank all the members of the families, for their invaluable contribution to this research; N. Akarsu, T. Ball, C. Black, P. Byers, T. Hamada, M. McAvoy, J. Power, J. Prendiville, and V. Wessagowit, for assistance in obtaining samples; and A. Bateman, at the Wellcome Trust Sanger Institute, for initial Pfam analysis of CMG2. M.E.C. and F.M.P. are supported by the Medical Research Council and the Ehlers-Danlos Support Group. A.S.F. is supported by the Swiss National Science Foundation (3100A0–100485). This work was supported by Institute of Cancer Research (U.K.).

Electronic-Database Information

Accession numbers and URLs for the data presented herein are as follows:

BLAST, http://www.ncbi.nlm.nih.gov/BLAST/ (for BLAST and tblastn, used in identification of *CMG2* paralogs and orthologs)

Center for Medical Genetics, http://research.marshfieldclinic.org/genetics/ (for identification of microsatellite markers)

ClustalW, http://www.ebi.ac.uk/clustalw/ (for alignment of human and orthologous CMG2 and TEM8 proteins)

Conserved Domain Database, http://www.ncbi.nlm.nih.gov/Structure/cdd/cdd.shtml (for analysis of cytoplasmic domain)

Ensembl, http://www.ensembl.org/ (for mouse cmg2 [Ensembl mouse peptide ENSMUSP00000046348] and fugu tem8 [Ensembl gene SINFRUG00000151577])

Expressed Sequence Tags Database, http://www.ncbi.nlm.nih.gov/dbEST/

GenBank, http://www.ncbi.nlm.nih.gov/Genbank/ (for human *CMG2* cDNA [accession number AK091721] and protein [accession number BAC03731], mouse cmg2 [accession number AAH03908], rat cmg2 [accession number XP_223745], human TEM8 [accession number Q9H6X2], mouse tem8 [accession number XP_132709], rat tem8 [accession number XP_232144], pig cytoplasmic domain [accession number AW657469], cow cytoplasmic domain [accession number AV599556], chicken cytoplasmic domain [accession number BI393979, and zebrafish cytoplasmic domain [accession number BI867612])

Human BLAT Search, http://genome.ucsc.edu/cgi-bin/hgBlat (for search engine used in alignment of *CMG2* cDNAs with genomic sequence)

MultAlin, http://prodes.toulouse.inra.fr/multalin/ (for alignment of cytoplasmic domains)

Online Mendelian Inheritance in Man (OMIM), http://www.ncbi.nlm.nih.gov/Omim/ (for JHF and ISH)

Pfam, http://www.sanger.ac.uk/Software/Pfam/ (for analysis of cytoplasmic domain)

Primer3, http://www-genome.wi.mit.edu/cgi-bin/primer/primer3_www.cgi (for design of chromosome 4q21 microsatellite markers and *CMG2* primers)

Prosite, http://us.expasy.org/prosite/ (for analysis of cytoplasmic domain)

UCSC Genome Bioinformatics, http://genome.ucsc.edu/ (for Human Genome Project Working Draft sequence and identification and position of microsatellite markers)

References

Allen PW (2001) Selected cases from the Arkadi M. Rywlin International Slide Seminar: hyaline fibromatosis. Adv Anat Pathol 8:173–178

Balci S, Kulacoglu S, Senoz O, Vargel I, Erk Y, Onder S, Gokoz A, Akarsu AN (2002) Juvenile hyaline fibromatosis in three

sibs from a consanguineous family: clinical, histopathological and immunohistochemical findings. Eur J Hum Genet 10:121

Bell SE, Mavilla A, Salazar R, Bayless KJ, Kanagala S, Maxwell SA, Davis GE (2001) Differential gene expression during capillary morphogenesis in 3D collagen matrices: regulated expression of genes involved in basement membrane matrix assembly, cell cycle progression, cellular differentiation and G-protein signalling. J Cell Sci 114:2755–2773

Bradley KA, Mogridge J, Mourez M, Collier RJ, Young JAT (2001) Identification of the cellular receptor for anthrax toxin. Nature 414:225–229

Breier F, Fang-Kircher S, Wolff K, Jurecka W (1997) Juvenile hyaline fibromatosis: impaired collagen metabolism in human skin fibroblasts. Arch Dis Child 77:436–440

Ganguly A, Rock MJ, Prockop DJ (1993) Conformation-sensitive gel electrophoresis for rapid detection of single-base differences in double-stranded PCR products and DNA fragments: evidence for solvent-induced bends in DNA heteroduplexes. Proc Natl Acad Sci USA 90:10325–10329

Glover MT, Lake BD, Atherton DJ (1991) Infantile systemic hyalinosis: newly recognised disorder of collagen? Pediatrics 87:228–234

——— (1992) Clinical, histologic and ultrastructural findings in two cases of infantile systemic hyalinosis. Pediatr Dermatol 9:255–258

Ishikawa H, Maeda H, Takamatsu H, Saito Y (1979) Systemic hyalinosis (juvenile hyaline fibromatosis): ultrastructure of the hyaline with particular reference to the cross-banded structure. Arch Dermatol Res 265:195–206

Iwata S, Horiuchi R, Maeda H, Ishikawa H (1980) Systemic hyalinosis or juvenile fibromatosis: ultrastructural and biochemical study of skin fibroblasts. Arch Dermatol Res 267: 115–121

Kayashima KI, Katagiri K, Shinkai H, Ono T (1994) Is juvenile hyaline fibromatosis a disease of type VI collagenosis? In: Ishibashi Y, Nakagawa H, Suzuki H (eds) Electron microscopy in dermatology—basic and clinical research. Elsevier Science, Amsterdam, pp 329–334

Keser G, Karabulut B, Oksel F, Calli C, Ustun E, Akalin T, Kocanaogullari H, Gumusdis G, Doganavsargil E (1999) Two siblings with juvenile hyaline fibromatosis: case reports and review of the literature. Clin Rheumatol 18: 248–252

Kitano Y, Horiki M, Aoki T, Sagami S (1972) Two cases of juvenile hyaline fibromatosis: some histological, electron microscopic, and tissue culture observations. Arch Dermatol 106:877–883

Landing BH, Nadorra R (1986) Infantile systemic hyalinosis: report of four cases of a disease fatal in infancy, apparently different from juvenile systemic hyalinosis. Pediatr Pathol 6: 55–79

Lubec B, Steinbert I, Breier F, Jurecka W, Pillwein K, Fang-Kircher S (1995) Skin collagen defects in a patient with juvenile hyaline fibromatosis. Arch Dis Child 73:246–248

Mancini GMS, Stojanov L, Willemsen R, Kleijer WJ, Huijmans JGM, van Diggelen OP, de Klerk JBC, Vuzevski VD, Oranje AP (1999) Juvenile hyaline fibromatosis clinical heterogeneity in three patients. Dermatology 198:18–25

Mayer-da-Silva A, Poiares-Baptista A, Guerra Rodrigo F, Teresa-Lopez M (1988) Juvenile hyaline fibromatosis: a histologic and histochemical study. Arch Pathol Lab Med 112:928–931

Nezelof C, Letourneux-Toromanoff B, Griscelli C, Girot R, Saudubray JM, Mozziconacci P (1978) La fibromatose disseminee douloureuse (hyalinose systemique). Arch Fr Pediatr 35:1063–1074

Rahman N, Dunstan M, Teare MD, Hanks S, Edkins SJ, Hughes J, Bignell GR, Mancini G, Kleijer W, Campbell M, Keser G, Black C, Williams N, Arbour L, Warman M, Superti-Furga A, Futreal PA, Pope FM (2002) The gene for juvenile hyaline fibromatosis maps to chromosome 4q21. Am J Hum Genet 71:975–980

Remberger K, Krieg T, Kunze D, Weinmann HM, Hubner G (1985) Fibromatosis hyalinica multiplex (juvenile hyaline fibromatosis), light microscopic, electron microscopic, immunohistochemical and biochemical findings. Cancer 56: 614–624

Richter D, Bode H, Debatin KM, Mohr W (1999) Juvenile hyaline fibromatosis. Monatsschr Kinderheilkd 147:473–476

Sahn EE, Salinas CF, Sens MA, Key J, Swiger FK, Holbrook KA (1994) Infantile systemic hyalinosis in a black infant. Pediatr Dermatol 11:52–60

Scobie HM, Rainey GJ, Bradley KA, Young JA (2003) Human capillary morphogenesis protein 2 functions as an anthrax toxin receptor. Proc Natl Acad Sci USA 100:5170–5174

St Croix B, Rago C, Velculescu V, Traverso G, Romans KE, Montgomery E, Lal A, Riggins GJ, Lengauer C, Vogelstein B, Kinzler KW (2000) Genes expressed in human tumor endothelium. Science 289:1197–1202

Stucki U, Spycher MA, Eich G, Rossi A, Sacher P, Steinmann, Superti-Furga A (2001) Infantile systemic hyalinosis in siblings: clinical report, biochemical and ultrastructural findings and review of the literature. Am J Med Genet 100:122–129